Appl Phys A (2012) 107:275–278
DOI 10.1007/s00339-012-6880-z

**Applied Physics A**
**Materials Science & Processing**

# Resonant Raman scattering of ZnS, ZnO, and ZnS/ZnO core/shell quantum dots

**A.G. Milekhin · N.A. Yeryukov · L.L. Sveshnikova · T.A. Duda · C. Himcinschi · E.I. Zenkevich · D.R.T. Zahn**

Received: 1 September 2011 / Accepted: 7 March 2012 / Published online: 20 March 2012


**Abstract** Resonant Raman scattering by optical phonon modes as well as their overtones was investigated in ZnS and ZnO quantum dots grown by the Langmuir–Blodgett technique. The in situ formation of ZnS/ZnO core/shell quantum dots was monitored by Raman spectroscopy during laser illumination.

A.G. Milekhin (✉) · N.A. Yeryukov · L.L. Sveshnikova · T.A. Duda
Institute of Semiconductor Physics, Lavrentjev av. 13, 630090 Novosibirsk, Russia
e-mail: milekhin@thermo.isp.nsc.ru

N.A. Yeryukov
e-mail: yeryukov@isp.nsc.ru

L.L. Sveshnikova
e-mail: svesh@thermo.isp.nsc.ru

T.A. Duda
e-mail: tanyaduda@gmail.com

A.G. Milekhin
Novosibirsk State University, Pirogov av. 2, 630090 Novosibirsk, Russia

C. Himcinschi
Institut für Theoretische Physik, TU Bergakademie Freiberg, Leipziger Str. 23, 09596 Freiberg, Germany
e-mail: himcinsc@physik.tu-freiberg.de

E.I. Zenkevich
Belarussian National Technical University, 220072 Minsk, Belarus
e-mail: zenkev@tut.by

D.R.T. Zahn
Semiconductor Physics, Chemnitz University of Technology, 09107 Chemnitz, Germany
e-mail: zahn@physik.tu-chemnitz.de

## 1 Introduction

II–VI semiconductor nanomaterials such as ZnS and ZnO quantum dots (QDs) having a wide band gap attract much attention due to their tremendous potential applications in ultraviolet optical and optoelectronic devices [1, 2]. The electron–phonon interaction influences the electronic and optical properties of the nanomaterials and consequently the device performance. Therefore the knowledge of the phonon spectra of nanomaterials is of a great importance. Several experimental techniques including methods of the wet chemistry [3–5] or combination of evaporation techniques with wet chemistry [6], colloidal chemistry [7–9], preparation of QDs in polymer matrices [10], sputtering techniques [11, 12], and sol–gel methods [13] are known to be used for the formation of ZnS and ZnO QDs. Among those the Langmuir–Blodgett (LB) technique is considered as a versatile, relatively simple, fast, and low-cost method for QD fabrication of II–VI and IV–VI materials with controllable QD areal density on different substrates [14–18]. It was established that ZnS and ZnO QDs grown by the LB technique are predominantly formed in a cubic and hexagonal symmetry, respectively [19]. Raman spectroscopy is one of the most powerful techniques for the investigation of phonon spectra of nanostructured materials. Most of the published data on the phonon spectra of QDs by a variety of fabrication methods were obtained by Raman scattering. Optical and surface optical phonon modes as well as multiphonon modes in CdS, PbS, CuS, and $Ag_2S$ QDs were observed in a number of resonant and non-resonant Raman experiments [3, 4, 6, 12].

In this paper we report on the fabrication of ZnS and ZnO QDs using the LB technique as well as on in situ formation of core/shell ZnS/ZnO QDs during laser annealing of the grown ZnS QDs and the study of their phonon spectra by means of Raman spectroscopy.

## 2 Experimental

The LB technology was used to prepare high quality films of Zn behenate on quartz and Si substrates covered by a 100 nm thick Au or Pt layer. The thickness of LB films under investigation was in the range of 100–400 monolayers. The reaction of the behenate with gaseous $H_2S$ (100 Torr, 22 °C) results in the formation of ZnS QDs. ZnS QD layers with nominal thicknesses of about 17–70 nm were obtained after removing the organic matrix by thermal annealing in an inert atmosphere at a temperature of 200 °C. ZnO QDs were formed as a result of annealing in air of either Zn behenate films or ZnS QDs at 600 °C.

Raman experiments were carried out using Dilor XY800, T64000, and Labram spectrometers in back-scattering geometries analyzing the non-polarized scattered light in a micro configuration at ambient conditions. The 514.5 and 325 nm lines of $Ar^+$ and HeCd lasers were used as excitation sources. The laser light with a power varying in the range of 0.4–40 mW was focused to a diameter of about 1 μm.

## 3 Results and discussion

The size of predominantly spherical ZnS QDs as determined from transmission electron microscopy and scanning electron microscopy experiments images is in the range of 2–6 nm. These data are in accordance with our previous results obtained for CdS, ZnS, and PbS QDs [20]. ZnO QDs have a half-spherical shape with a base size of about 40 nm and a QD height of about 4 nm.

The energies of interband transitions in ZnO and ZnS QDs are about 3.3 and 4 eV, respectively, and are close to or exceed the direct band gap energies of the corresponding bulk material [18]. This makes non-resonant (*e.g.* at $\lambda = 514.5$ nm (2.41 eV)) and near-resonant (at $\lambda = 325$ nm (3.82 eV)) Raman scattering measurements of the QDs possible.

Figure 1 shows the non-resonant Raman scattering spectra of ZnS and ZnO QDs measured with $\lambda = 514.5$ nm at 300 K after removal of the organic matrix. Since ZnS QDs refer to the nanostructures having the cubic symmetry, scattering by *LO* optical phonons in the QDs should contribute predominantly to the Raman spectra. Therefore, the peak at about 348 $cm^{-1}$ is assigned to the *LO* phonon mode. A weaker feature at about 220 $cm^{-1}$ is attributed to second-order Raman scattering [21]. ZnO QDs under investigation have a wurtzite crystal structure [19] and demonstrate in the non-resonant Raman spectra a pronounced vibrational mode at 440 $cm^{-1}$ and a relatively broad peak centered at 583 $cm^{-1}$ assigned to the $E_2$(high) mode and the contribution of $A_1(LO)$ and/or $E_1(LO)$ phonons in the QDs, respectively. A weak feature at 335 $cm^{-1}$ is due to a second-order

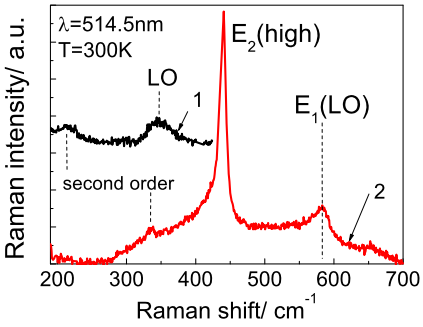


**Fig. 1** Non-resonant Raman spectra of (**1**) ZnS and (**2**) ZnO QDs measured with $\lambda = 514.5$ nm and a laser power of 10 mW

Raman scattering process in ZnO [22]. These observations are similar to the results obtained for ZnO QDs with a diameter of 20 nm prepared by a wet-chemistry method [4].

Note that the QDs are transparent for the laser light with $\lambda = 514.5$ nm and, therefore, neither any shift of the phonon frequency positions nor structural changes in the QDs due to the laser heating was observed under these non-resonant conditions despite the fact that the laser power was varied in the range from 10 to 40 mW.

Resonant Raman spectra of ZnS QDs with a nominal thickness of 70 nm (Fig. 2a) measured with laser wavelength of 325 nm demonstrate strongly enhanced (two orders of magnitude) Raman scattering by *LO* phonon modes at 348 $cm^{-1}$ and its overtone at doubled frequency. In addition, new weaker features were observed at 302, 431 and 643 $cm^{-1}$ the frequency positions of which were derived from the best fit of the experimental spectrum using Lorentzian curves. The feature at 302 $cm^{-1}$ is situated between the frequency positions of *LO* and *TO* (273 $cm^{-1}$) phonons at the center of the Brillouin zone ($\Gamma$ point) of ZnS. Typically, surface optical (*SO*) modes which exist near QD surface and decay exponentially away from the surface are responsible for appearance of the modes located between the *LO* and *TO* frequency positions. However, according to infrared reflection measurements performed on the ZnS nanostructures (not shown here) the frequency position of the *SO* phonon corresponds to a value of 330 $cm^{-1}$ which agrees well with calculated and experimental data obtained earlier for ZnS QDs [6]. This value differs from the frequency position of the observed feature (302 $cm^{-1}$). Therefore, it was attributed to the *TO* phonon mode from the *X* point of the Brillouin zone [23]. This mode is normally prohibited by Raman selection rules for cubic crystals. However, the weakening of selection rules in QDs can promote the observation of "prohibited" lines in Raman spectra. Analogously, the vibrational modes seen at 431 and 643 $cm^{-1}$ were attributed to the second-order Raman scattering by $LA(X)$ or $LA(L)$ phonons and to the combinational mode $(LO(\Gamma) + TO(X))$ [23].

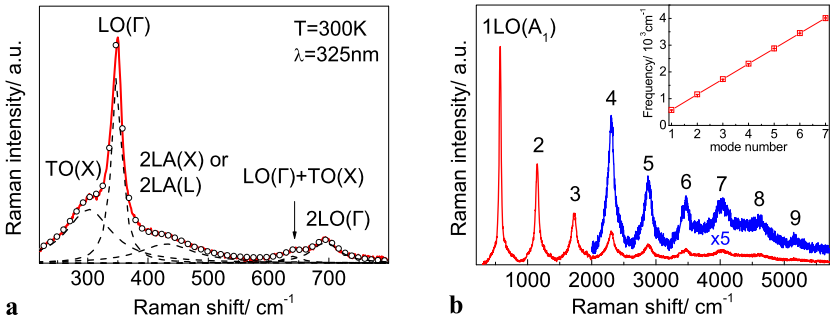


**Fig. 2** Resonant UV Raman spectra of (**a**) ZnS and (**b**) ZnO QDs measured with $\lambda = 325$ nm and a laser power of 1.5 mW. The *numbers in the right panel* indicate the corresponding overtones of $LO(A_1)$ phonon mode. The *inset* shows the frequency position of overtones vs. the overtone order

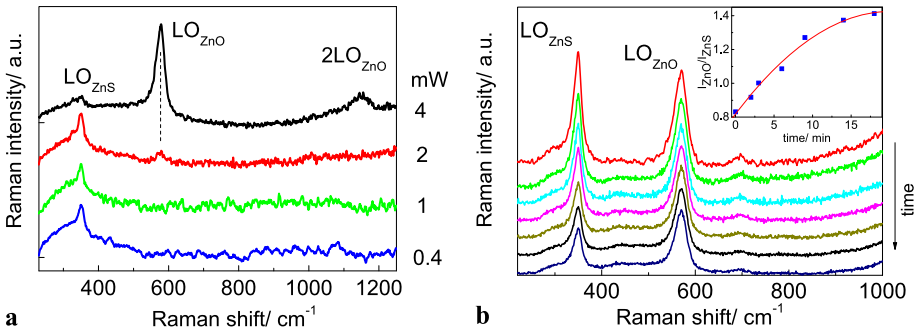


**Fig. 3** (**a**) Raman spectra of ZnS QDs measured during oxidation process under laser illumination with 325 nm during 15 s with different laser power, (**b**) time evolution of Raman spectra of ZnS/ZnO core/shell QDs measured with 325 nm during 60 s and a laser power of 3 mW

Figure 2b shows the resonant Raman spectrum of ZnO QDs with a nominal thickness of 70 nm. The most prominent peak at 576 cm$^{-1}$ indicated as $1LO(A_1)$ is due to first-order Raman scattering by *LO* phonons of $A_1$ symmetry [4]. A large number of periodical peak repetitions is attributed to multiple-phonon Raman scattering (up to ninth order) and indicates the very high crystalline quality of the fabricated nanostructures. To the best of our knowledge, multiphonon *LO* modes in ZnO QDs were observed up to eighth order at low temperature (77 K) while a strong band edge free excitonic photoluminescence near 4000 cm$^{-1}$ prevents the observation of multiphonon modes at room temperature [12]. In our case, this photoluminescence is suppressed most probably by defect states at the QD surfaces as well as by minimization of laser excitation power and spectrometer slits. As one can see from the inset to Fig. 2b, the frequency position of the $n$th overtone is well described by the formula $\omega_n = n \cdot \omega(LO(A_1))$.

The information on the phonon spectra of ZnO QDs was used to explain the evolution of resonant Raman spectra of ZnS QDs with laser power density and illumination time. Figure 3a shows the Raman spectra of ZnS QDs measured with different laser power (from 0.4 to 4 mW) with accumulation time of 15 seconds. One can see that at a low laser excitation power (up to 1 mW) the Raman spectra evidence only the *LO* phonon mode near 350 cm$^{-1}$ originating from ZnS QDs. A higher laser excitation power (above 1 mW) causes the appearance of a peak at about 576 cm$^{-1}$ which is attributed to the $LO(A_1)$ phonon mode from a ZnO shell formed most probably due to a partial oxidation of the ZnS QDs. Its intensity ($I_{\mathrm{ZnO}}$) increases with increasing the laser power while the intensity of *LO* phonon peak from the ZnS core ($I_{\mathrm{ZnS}}$) decreases simultaneously. Raman spectra measured with 4 mW demonstrate the appearance of the *LO* phonon overtone from the ZnO shell (denoted in Fig. 3a as $2LO_{\mathrm{ZnO}}$).

Time evolution of Raman spectra of ZnS/ZnO core/shell structure under laser illumination (3 mW) is shown in Fig. 3b. One can see that the Raman spectrum measured at a laser power of 3 mW during the first 60 s reveals besides the *LO* phonon mode in the ZnS core seen at 350 cm$^{-1}$ the feature at 576 cm$^{-1}$ due to Raman scattering by the $LO(A_1)$ phonon in the ZnO shell. One can see from Fig. 3b that the intensity of both modes decreases with time while their ratio $I_{\mathrm{ZnO}}/I_{\mathrm{ZnS}}$ increases. The first issue indicates a partial amorphization of the nanostructure under intensive laser illumination while the second one evidences increasing thickness of the ZnO shell. The evolution of the intensity ratio of the phonon modes in the shell and the core shown in the inset to Fig. 3b shows a trend towards saturation after 10 minutes of laser illumination. This means that the ZnO shell prevents further oxidation of the ZnS core. No remarkable shift of the phonon modes induced by the phonon confinement in either ZnS or ZnO was observed which one could expect for thin ZnO shells of small ZnS core. This can be explained by a rather flat dispersion of the optical phonons in ZnO and ZnS [23] and a broad size distribution of the QDs.

## 4 Conclusion

We demonstrate the successful growth of ZnS and ZnO QD arrays using LB technology. Non-resonant and resonant Raman scattering by *LO* phonons in ZnS and ZnO QDs is observed. Multiple-phonon Raman scattering in ZnS and ZnO QDs up to second and ninth order, respectively, confirms a high crystalline quality of the QDs grown and evidences a strong electron–phonon interaction in the QDs. Time evolution of Raman spectra under laser illumination allows the monitoring of oxidation processes of ZnS nanostructures resulting in the formation of ZnS/ZnO core/shell QDs.

**Acknowledgements** This work was supported in part by the Russian Foundation for Basic Research (grants RFBR-DFG 11-02-91348, 11-02-90427-Ukr_a), Siberian Branch of Russian Academy of Sciences (joint grant with NAS of the Republic of Belarus n.9), Deutsche Forschungsgemeinschaft (grant Za 146/22-1) and the International Research Training Group (Internationales Graduiertenkolleg, GRK 1215) "Materials and Concepts for Advanced Interconnects".

## References

1. D.A. Gaul, W.S. Rees Jr., Adv. Mater. **12**, 935 (2000)
2. M.A. Hasse, J. Qui, J.M. De Puydt, H. Cheng, Appl. Phys. Lett. **59**, 1272 (1991)
3. S. Dhara, A.K. Arora, S. Berac, J. Ghatak, J. Raman Spectrosc. **41**, 1102–1105 (2010)
4. K.A. Alim, V.A. Fonoberov, A.A. Balandin, Appl. Phys. Lett. **86**, 053103 (2005)
5. S.S. Kurbanov, G.N. Panin, T.W. Kim, T.W. Kang, Journal of. Luminescence **129**, 1099 (2009)
6. J. Xu, H. Mao, Y. Sun, Y. Du, J. Vac. Sci. Technol. B **15**, 1465 (1997)
7. R. Rossetti, R. Hull, J.M. Gibson, L.E. Brus, J. Chem. Phys. **82**, 552 (1985)
8. J. Nanda, D.D. Sarma, J. Appl. Phys. **90**, 2504 (2001)
9. R.D. Yang, S. Tripathy, Y. Li, H.-J. Sue, Chem. Phys. Lett. **411**, 150–154 (2005)
10. Y. Yang, J. Huang, S. Liua, J. Shen, J. Mater. Chem. **7**, 131–133 (1997)
11. J. Antony, X.B. Chen, J. Morrison, L. Bergman, Y. Qiang, D.E. McCready, M.H. Engelhard, Appl. Phys. Lett. **87**, 241917 (2005)
12. B. Kumar, H. Gong, S.Y. Chow, S. Tripathy, Y. Hua, Appl. Phys. Lett. **89**, 071922 (2006)
13. H.-M. Cheng, K.-F. Lin, H.-C. Hsu, W.-F. Hsieh, Appl. Phys. Lett. **88**, 261909 (2006)
14. G. Zylberajch, A. Ruaudel-Teixier, A. Barraud, Thin Solid Films **178**, 535 (1989)
15. M. Seidl, M. Schurr, A. Brugger, E. Volz, H. Voit, Appl. Phys. A **68**, 81–85 (1999)
16. A.G. Milekhin, L.L. Sveshnikova, T.A. Duda, N.V. Surovtsev, S.V. Adichtchev, D.R.T. Zahn, JETP Lett. **88**, 799 (2008)
17. M. Parhizkar, N. Kumar, P.K. Nayak, S.S. Talwar, S.S. Major, R.S. Srinivasa, Colloids Surf. A, Physicochem. Eng. Asp. **257–258**, 405–410 (2005)
18. A. Milekhin, L. Sveshnikova, T. Duda, N. Surovtsev, S. Adichtchev, D.R.T. Zahn, J. Vac. Sci. Technol. B **28**(4), C5E22–C5E24 (2010)
19. A.G. Milekhin, L.L. Sveshnikova, T.A. Duda, N.V. Surovtsev, S.V. Adichtchev, Y.M. Azhniuk, C. Himcinschi, M. Kehr, D.R.T. Zahn, J. Phys. Conf. Ser. **245**, 012045-1-4 (2010)
20. A.G. Milekhin, L.L. Sveshnikova, S.M. Repinsky, A.K. Gutakovsky, M. Friedrich, D.R.T. Zahn, Thin Solid Films **422**(1–2), 200–204 (2002)
21. O. Brafman, S.S. Mitra, Phys. Rev. **171**, 931 (1968)
22. T.C. Damen, S.P.S. Porto, B. Tell, Phys. Rev. **142**, 570 (1966)
23. O. Madelung (ed.), *Landolt–Bornstein Tables 1999,* New Series, Group III, v. 41B (Springer, Berlin, 1999)